Prayogik Rasayan

Transition Metal's Hydroxide for Electrochemical Water Oxidation Reaction

Subrata Kundu[†‡*]

[†] Electrochemical Process Engineering (EPE) Division, CSIR-Central Electrochemical Research Institute (CECRI), Karaikudi-630003, Tamil Nadu, India.
[‡] Academy of Scientific and Innovative Research (AcSIR), Ghaziabad-201002, India.

* E-mail: skundu,cecri@csir.res.in and kundu.subrata@gmail.com

Received: January 05, 2026 | Accepted: March 10, 2026 | Published online: March 31, 2026

Abstract

Hydrogen has a high energy density and is good alternative for carbon-based fuels. Eectrochemical Water splitting provides a green method for hydrogen production. Though Pt, RuO_2, and IrO_2 are excellent electrocatalysts for HER and OER, their costly and scarce hinder their application for water splitting. This review focuses advance in transition metal hydroxides for electrochemical water splitting, catalysts, mechanisms, and approach for improving the water splitting-kinetics.

Keywords:

Hydrogen; OER; HER; overpotential; Tafel slope; Hydroxide; LDHs.

1. Introduction

Utilizing a large amount of carbon-based fuels has become crucial due to the continued growth of globalization and the need to meet energy demands (1-4). A significant amount of CO_2 (37.11 billion ton/year) is released into the atmosphere by the widespread use of these carbon fuels to generate energy, which has a detrimental effect on our climate by increasing Earth's temperature. Furthermore, since these carbon-based fuel stocks are finite, it is imperative to create a reliable alternative energy source that can effectively supply these high energy demands while guaranteeing that these energy sources are non-renewable. With a high specific energy density of 142 KJ/mol, hydrogen has considered as an major alternative energy source (5-8). Hydrogen can be produced efficiently from different processes, such as Electrochemical and photochemical water splitting, hydrolysis of metal hydrides, and steam reforming of hydrocarbons. Nevertheless, each of these processes having its own merits and demerits. For example, producing hydrogen throguh steam reforming processes it releases huge quantity of greenhouse gases to the environment, and photochemical water splitting has poor efficiency towards green hydrogen production (9–12). Because of its ease of use and environmental friendliness-as long as the energy input is derived from renewable sources-hydrogen generation using water electrolysis has garnered significant interest from academics. The Hydrogen Evolution

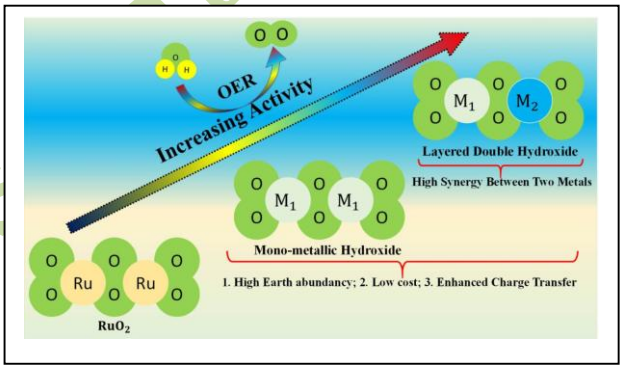

Reaction (HER), and Oxygen Evolution Reaction (OER) at the cathode and anode in the overall cell arrangement are the two half-cell reactions that make up electrocatalytic water splitting (13). The HER and OER in electrocatalytic water splitting proceed via two-and four-electron transfer mechanisms, respectively, with pathways that vary according to the electrolyte pH. Given the intrinsically sluggish kinetics of both half-reactions, efficient catalysts are essential at both anode and cathode to accelerate overall water splitting. To date, platinum remains the benchmark HER catalyst, while noble metal oxides such as RuO_2, and IrO_2 set the performance standards for OER (14). However, the synthesis of hydrogen is expensive due to the dependence on these rare noble metals. As a result, there has been a substantial focus on developing low-cost, earth-abundant 3d transition metals. Long-term water electrolysis has shown the efficacy of a number of compounds based on 3d transition metals, such as hydroxides, oxides, chalcogenides, and pnictides (15–19). Metal hydroxides made from three-dimensional transition metals stand out among other transition metal-based electrocatalysts because of their non-toxicity, simplicity in synthesis, ideal shape, and remarkable durability in alkaline

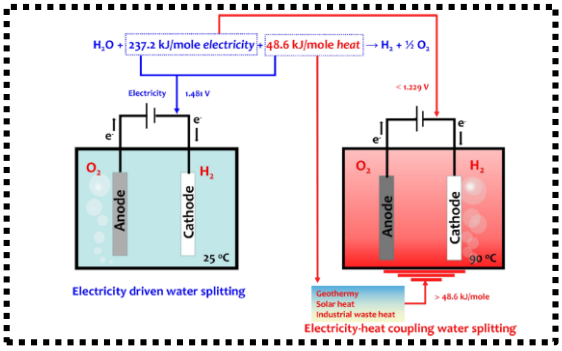

Figure 1: *Electricity heat coupling water splitting. Reproduced with permission from reference number 25, American chemical society, 2022.*

systems (20). Despite the high catalytic performance observed for metal hydroxide-based materials for OER, there are a number of challenges that need to be addressed for the development of these catalysts for efficient application. Firstly, the catalysts are known to undergo structural deterioration or dissolution during prolonged anodic potentials. Secondly, the inherently low electrical conductivity observed for these catalysts often requires additional support for efficient application. Thirdly, the surface reconstruction that occurs during the course of the electrochemical reaction often raises questions regarding the active phase for the electrochemical reaction. Lastly, most electrochemical studies are carried out on a laboratory scale at relatively low current densities. Rational design of highly selective electrocatalysts, underpinned by comprehensive mechanistic insights, holds the key to maximizing hydrogen evolution efficiency (21). This chapter discusses both photocatalytic and electrocatalytic water splitting for hydrogen production, covering foundational concepts, recent advancements, and future prospects for large-scale hydrogen generation (22-27).

2. Thermodynamic Barriers and Kinetic Challenges in Water Electrolysis

The basic idea behind water splitting is to use electricity from external sources to split a water molecule into hydrogen and oxygen (28-31).To enable water splitting with the least amount of energy possible, an effective electrocatalyst is necessary. Electrocatalytic water splitting frequently necessitates a significant energy input because of the complex mechanistic nature of the half-cell reaction. The remarkable thermal stability of water molecules, which have an octet electronic configuration, is the chemical explanation for this substantial energy required for water electrolysis (32-35). Because of the exceptional stability of the H_2O molecule, the reverse process requires significant energy input, even if the synthesis of H_2O from two hydrogen atoms and one oxygen atom is energetically beneficial (leading to energy release). The half-cell reaction for the overall water splitting can be expressed as follows:

Anode: $H_2O = 1/2O_2 + 2H^+ + 2e^-$ ..... (i) (E_{O_2/H_2O}=1.23 V vs RHE)

Cathode: $2H^+ + 2e^- = H_2$ .....(ii) (E_{H^+/H_2}= 0 V vs RHE)

The combined cell potential (E_{cell}) amounts to 1.23 Volt against reversible hydrogen electrode (RHE). Consequently, the potential for water splitting, derived thermodynamically, is 1.23 V, remains constant regardless of the electrolyte utilized or the pH of the solution (36-42). The change in Gibbs free energy (ΔG) for water is significantly positive, specifically +237 kJ mol^{-1}(41-42). This substantial positive ΔG indicates that the reaction is non-spontaneous. From a comprehensive thermodynamic perspective, it's noteworthy to reflect on the following equation:

$$\Delta G = \Delta H - T\Delta S \text{ ..... (iii)}$$

where ΔH represents the total changes in enthalpy, ΔS signifies the entropic term, and T denotes the absolute temperature measured in kelvins (43). In the context of water splitting, it is noteworthy that the entropic term is positive, suggesting that this positive value could support the water splitting process (44-45). However, in practical scenarios, the highly stable nature of water results in a significantly positive overall enthalpic term, which ultimately dominates over the entropic term, leading to a positive ΔG overall (46-48).

Applying a voltage of 1.23 V vs RHE is expected to facilitate the splitting of water molecules when taking into account the kinetic side of water splitting by electrochemical methods. However, in practice, the thermodynamically computed potential value cannot be used to separate water molecules; instead, an extra potential known as "overpotential" is required (49-50).The overpotential required for water electrolysis arises predominantly from the intrinsically sluggish kinetics of the half-cell reactions, namely the HER and OER which are entirely neglected in purely thermodynamic potential calculations. Beyond these kinetic limitations, an additional thermochemical factor emerges, the enthalphy for vaporizing liquid water to steam under adiabatic conditions, which further elevates the minimum energy input for practical H_2 production (51). To effectively maintain the study of water splitting, it is essential to supply both electrical and thermal energy at the same time. Therefore, the overall energetics of the water-splitting reaction can be expressed as follows:

H_2O + 237.2 KJ mol^{-1} (ΔG) +48.6 KJ mol^{-1} (heat) = H_2 + ½ O_2..... (iv)

The heat transmitted, expressed as TΔS (where T is the absolute temperature and ΔS is the change in entropy), is 48.6 KJ/mol, but the free energy change for the splitting of water is 237.2 KJ/mol. As shown in Figure 1, it is therefore crucial to supply an additional overpotential for the phase transformation in addition to the energy needed to separate water molecules (25). The potential that results from taking this temperature impact into consideration is known as the thermoneutral potential (E_{tneut}), and it can be written as follows:

$$E_{tneut} = \frac{(\Delta G + T\Delta S)}{2F} \text{.....(v)}$$

In practice, the required energy input is not the Gibbs free energy change of 237.2 kJ mol-1 (Corresponding to 1.23 V vs.

RHE) but rather the enthalpy changes of 285.8 kJ mol-1 necessitating a cell voltage of 1.481 V vs. RHE.

3. Mechanism of HER and OER

The electrochemical performance of catalysts in Oxygen Evolution Reaction is commonly examined through several parameters that offer valuable information on catalyst performance, kinetics, intrinsic efficiency, etc. These parameters are extremely useful in understanding catalyst performance comprehensively and comparing various electrocatalysts (5).

3.1. Overpotential:

The overpotential value is a major parameter used for measuring the efficiency of a catalyst for the Oxygen Evolution Reaction. The additional potential value is necessary for the completion of the Oxygen Evolution Reaction at a given current density (usually 10 mA cm^{-2}). A lower overpotential value means that the catalyst is efficient because less additional energy is required for the completion of the electrochemical reaction (51-52).

3.2. Tafel Slope:

The Tafel slope helps in understanding the kinetics of the Oxygen Evolution Reaction and the possible mechanisms that occur during the electrochemical reaction. It is usually calculated from the linear region of the Tafel plot (overpotential-current density). A lower Tafel slope means faster kinetics for the electrochemical reaction.

3.3. Electrochemically Active Surface Area (ECSA):

The electrochemically active surface area (ECSA) is the catalytically active surface area for the reaction. The electrochemically active surface area is usually calculated from the double-layer capacitance data using cyclic voltammetry in a non-faradaic region. The electrochemically active surface area is a measure of the number of active sites available for the reaction. Therefore, the electrochemically active surface area is usually high for a material with high catalytic activity.

3.4. Turnover Frequency (TOF):

Turnover frequency (TOF) is a measure that represents the inherent catalytic capability of a given material by determining the number of reaction events per active site per unit time during the Oxygen Evolution Reaction. TOF is different from current density in that the former normalizes the activity in terms of the number of active sites.

3.5. Stability:

Stability matters a lot for OER catalyst to work well in real electrolyzers. We test it using chronopotentiometry (Change in potential with respect to the time) or Chronoamperometry (Change in the current with respect to the time) in basic solution. A high performance catalyst keeps voltage steady or current high for 24-100 hours at 10 mA/cm^2 like voltage rise under 5mV/hours. Always fix resistance drops, check true electrochemical active surface area, and use scans (LSV) before after the stability, examine surface with physiochemical (XPS, FE-SEM) characterizations to spot changes.

4. Mechanism of HER and OER

Turning to the mechanism of OER, it is important to point out that the mechanistic pathways are more intricate compared to those in HER (53-55). The oxygen evolution reaction (OER) entails a demanding four-electron, four-proton transfer process, which imposes significant kinetic barriers and profoundly impacts the efficiency of anodic processes in alkaline electrolysers. These inherent mechanistic complexities necessitate highly active OER electrocatalysts to enable practical deployment and commercialization. Mechanistic pathways vary distinctly with electrolyte pH, with alkaline conditions favouring hydroxide-mediated nucleophilic steps, the core sequence from active site hydroxylation to O-O coupling and release-is outlines in Equations (vi)-(xi) (S= catalytic centre), as depicted schematically in **Figure 2.**

$$S + H_2O \xrightarrow{\text{Acid}} S\text{-}OH + H^+ + e^- \quad \ldots\ldots\ldots \text{(vi)}$$

$$S\text{-}OH \xrightarrow{\text{Acid}} S\text{-}O + H^+ + e^- \quad \ldots\ldots\ldots \text{(vii)}$$

$$2S\text{-}O \xrightarrow{\text{Acid}} 2S + O_2 \quad \ldots\ldots\ldots \text{(viii)}$$

$$S + OH^- \xrightarrow{\text{Alkali}} S\text{-}OH + H^+ + e^- \quad \ldots\ldots\ldots \text{(ix)}$$

$$S\text{-}OH + OH^- \xrightarrow{\text{Alkali}} S\text{-}O + H_2O + e^- \quad \ldots\ldots\ldots \text{(x)}$$

$$2S\text{-}O \xrightarrow{\text{Alkali}} 2S + O_2 \quad \ldots\ldots\ldots \text{(xi)}$$

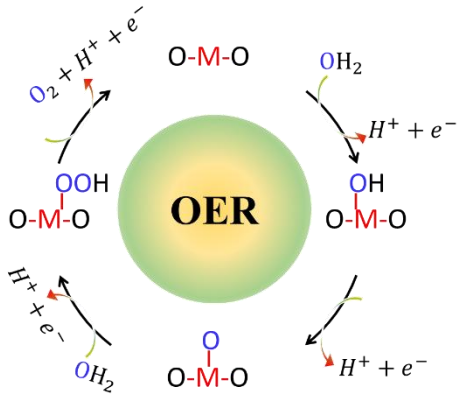

Figure 2: *Mechanistic pathways for OER in alkaline condition.*

In an alkaline setting, subsequent reactions take place following the establishment of the M-OH bond, either leading to the creation of a metal oxide (M-O) or a metal oxyhydroxide (M-OOH) intermediate (56-58). Among the various proposed mechanisms for the OER, the identity of the rate-determining step (RDS) fundamentally governs the required overpotential. Thus, rational electrocatalyst design must prioritize the formation of the S-O bond with an optimal binding energy, neither excessively strong nor week to minimize the thermodynamic barrier and enhance turnover rates.

5. Significance of Electronic Structure in Electrocatalysis

The electrical configuration of the reactive species and active metal sites has a significant impact on the efficient creation of an electrocatalyst for different purposes. Throughout the catalytic cycle, adsorption and desorption work together in a heterogeneous electrocatalytic reaction. The binding energy of adsorbed intermediates on catalytically active sites governs electrocatalytic efficiency. Stronger binding strengthens the metal-intermediate bond (e.g., M–O) during OER, enhancing resilience, which may cause problems in the latter stage of desorption (59-60). Therefore, the M–O bond's electrical structure is essential to the reaction's kinetics. The Sabatier principle dictates that optimal electrocatalysts exhibit balanced free energy for metal-intermediate formation ($\Delta G_{RI} \approx 0$) producing a relationship resembling a volcano-shaped plot (see Figure 3a). Several factors, detailed below, govern the energetics of the electrochemical reaction.

Ongoing research targets efficient electrocatalysts, as the high activation barrier renders water splitting (and its reverse) thermodynamically quasi-irreversible. The stable octet electron configuration that H_2O and O_2 molecules display is the cause of this barrier. Furthermore, the source of this higher kinetic barrier can be easily predicted by examining the molecular orbital (MO) diagram. The large HOMO–LUMO gap partly drives high energy needs in electrocatalysis, with an additional ~1 eV cost from spin-state shifts in the H_2O-to-O_2 (or reverse) cycle. (61-62).

In the H_2O–O_2–H_2 system, metal-site electronic structure governs reaction kinetics alongside intermediate energetics-proton-coupled electron transfer (PCET) drives stepwise metal redox across each OER step. Among these processes, OER

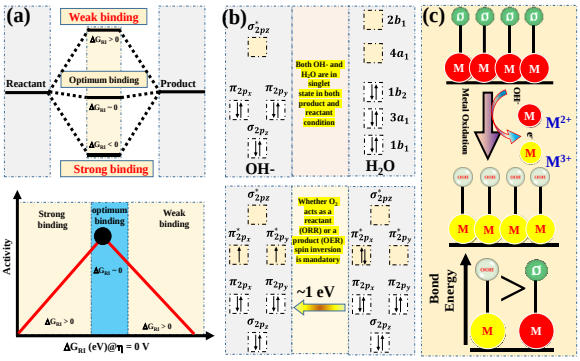

Figure 3: *(a) illustration of the optimal electrocatalytic activity in a heterogeneous catalytic system according to the Sabatier Principle; (b) molecular orbital diagram for H_2O, O_2, and OH-ions; and (c) schematic representation of the bond energetics of M-O bonds in different stages of the OER catalytic cycle.*

and ORR both require metal oxidation from +2 to +3, facilitating the conversion of M–O (in OER) or M–O_2 (in ORR) to M–OOH. Therefore, metals must have a significant reducing capacity or a predisposition for oxidation in order for the OER to occur successfully. Among the 3d transition metals, nickel (Ni) is acknowledged as the most suitable option for OER and occasionally for ORR as well. Ni is a great option for both OER and ORR due to its remarkable reduction capacity and effective self-oxidation process. Furthermore, iron (Fe) and cobalt (Co) are favorable metals for water splitting applications due to their high reducing properties (63-64).

The d-band center (E_d) of active metal cations serves as a cornerstone electronic descriptor in designing efficient oxygen electrocatalysts, primarily dictating the adsorption strength of OH intermediates. According to d-band center theory, the position of Ed relative to the Fermi level (E_F) correlates directly with bonding, E_d closer to E_f enhances overlap with OH antibonding orbitals, strengthening interactions, conversely, downward dhifts reducte it. In 3d dimensional transition metal-based systems, electronic filling determines this positioning-metal ions with more than half-filled d-orbitals (d^6-d^{10}) shift E_d upward toward E_F, while those below (d^1-d^5) shift it downward. Thus, Co^{2+} (d^7) and Ni^{2+} (d^8) achieve Sabatier-ptimal O*H binding, outperforming other 3d metals in OER activity. Beyond adsorption, O_2 desorption kinetics profoundly influences the operating current-voltage characteristics. (65-66). Hence, the M-O bond energy ($E^n_{M\text{-}O}$, where n is the metal oxidation state) and the electronic structure in the higher oxidation states are key. Local electronic effects further govern O_2 desorption (Figure 3c): electronic-rich anions (e.g., S^{2-}, Se^{2-}) promote it via intensified 3d-2p repulsion from anion-to-metal electron donation. This extends to bimetallics, eg., Karmakar et at., showed Fe_{2+} doped Ni_3Se_4 boosts OER via electron transfer from reducing Fe^{2+} to Ni^{3+}, amplifying repulstion. Transition metal catalyst excel in OER due to optimal d-configurations enabling 3d-2p repulsion-aided O_2 release. Notably, Ni^{2+} (d^8) favours M-OH formation, facilitating O_2 detachment from Ni sites and yielding marked alkaline OER gains.

6. Replacing Noble-catalyst to Non-Precious Hydroxide Electrocatalyst for water splitting

To mitigate dependence on noble-metal electrocatalysts, non-precious 3d transition metal chalcogenides, oxides, hydroxides, and phosphides have emerged as highly active for alkaline water splitting, exhibiting robust stability. Notably, their hydroxide phases deliver superior bifunctional OER/HER performance at reduced over potentials. Hydroxides offer key advantages such as facile synthesis, octahedral metal coordination, and tunable electronic structure. Iron-group metals (Fe, Co, Ni) excel in OER owing to optimal d-electronic configurations enabling 3d-2p repulsion for efficient O_2 desorption.

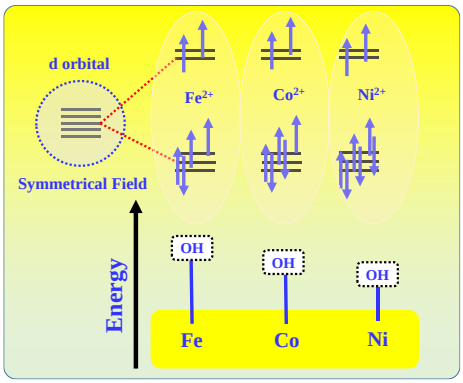

Figure 4: *a) electronic configuration of M^{2+} ions from iron group elements and b) The corresponding requirement of energy to form M-OH bonds during OER in alkali.*

As shown in Figure 4, M-OH formation controlled by on their electronics, Ni^{2+} (d^8) particularly favors it, accelerating subsequent O_2 release and boosting alkaline OER performance (66).

During alkaline water oxidation, the catalytic cycle commonly proceeds through the formation of a metal-hydroperoxo (M-OOH) intermediate generated by direct nucleophile attack of hydroxide ions on a high-valent metal-oxo (M-O) species. This pathway is particularly accessible in transition-metal hydroxides because their local coordination environment is structurally and electronically similar to that of the in-situ formed (oxy) hydroxide phases, which minimizes lattice rearrangement during redox cycling and facilitates rapid generation of active sites. Building on these mechanistic advantages, the following section critically examines the electrocatalytic performance of hydroxide-based materials toward overall water splitting, with emphasis on oxygen evolution activity, structure-property relationships, and emerging design strategies in this rapidly evolving field.

6.1. Mono-metallic hydroxides in water splitting reactions

Recent interest has surged in using abundant, cost-effective 3d transition metal electrocatalyst for overall water splitting. Monometallic hydroxide such as $Ni(OH)_2$ and $Co(OH)_2$, these materials display outstanding OER/HER performance, specifically in alkaline media, thanks to their distinctive two-dimensional structures. Cobalt and Nickel display two crystalline phases at ambient temperature: the β and α-phase. To date, most characterized monometallic hydroxides have exhibited excellent OER activity. However, these bare hydroxides have not achieved HER activity under the same alkaline conditions. The absence of HER activity can be attributed to i) low electrical conductivity; ii) the inadequate active sites for hydrogen adsorption; and iii) the inability of single metallic systems to effectively dissociate water molecules in alkaline environments, as discussed earlier. Since this chapter primarily focuses on the total water splitting reaction, address recent advancements in hydroxides that enable overall splitting, rather than those that excel solely in HER or OER. In recent times, different strategies have been introduced to overcome these limitations and enhance the HER activity of pristine monometallic hydroxides through the doping of external cations, which has led to significant improvements in alkaline HER performance with minimal applied potential.

Qiao et al., described a simple intial synthesis of iron-doped-$Ni(OH)_2$ nanopyramids through chemical deposition, subsequently anionic exchange of the C_2O_4 unit from FeNi-C_2O_4/NF with OH^- ions (Figure 6) (44). The FeNi-C_2O_4/NF template was prepared solvothermally using mixture of nitrate salts of Ni and Fe as metal ion sources, with oxalic acid serving as the framework template. This templates was then treated with 0.1 M NaOH solutions for 12 hours, to produce Fe-doped $Ni(OH)_2$, which was served as water splitting catalyst. The high intrinsic activity of prepared catalyst combined with its unique morphology on the 3D conductive substrate, enabled significant water-splitting performance in a solution of 1 M KOH (67). The optimial Fe-doped $Ni(OH)_2$ material showed a low overpotential of 218 mV (OER) and 121 mV (HER) conditions at 10 mA/cm^2, compared to 313 mV/207 mV overpotential for OER/HER conditions, respectively.

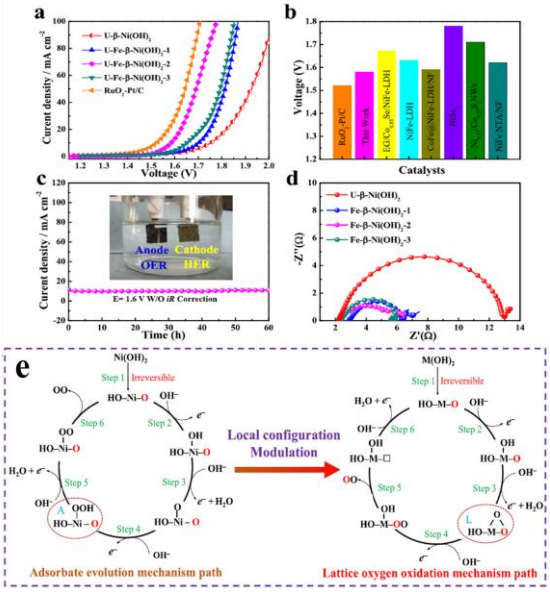

Figure 5: *Synthetic strategies followed for the synthesis of U-Fe-β-Ni(OH)$_2$/NF. Reproduced with permission from reference number 44, American Chemical Society, 2020.*

Overpotentials were measured in a three-electrode configuration, revealing Fe-doping's profound influence on interfacial charge transfer kinetics. The electrocatalyst exhibited bifunctional excellence, requiring only 1.58 V in a two-electrode alkaine electrolyzer to drive 10 mA cm^{-2} couple with >60h durability (Figure 8a-d). pH-dependent LSV (pH 12.5-14) showed enhanced sensitivity in the doped system versus pristine $Ni(OH)_2$, attribute to pH-driven surface reconstruction exposing deeper active regions.

DFT computations elucidate the mechanism shift, Fe activates lattice oxygen, localizing electronic charge distribution at Fe-O bonds and transitioning from adsorbate evolution mechanism

(AEM) to lattice oxygen oxidation mechanism (LOM) (Figure 8e). Ren et al., similarly prepared hierarchical porous FeNiOH/NF hydrothermally in $(NH_4)_2S_2O_8$, yielding η_{OER}= 271 mV and η_{HER}=166 mV to attain 20 mA cm^{-2}. Tafel analysis (FeNiOH/NF: 64 mV dec^{-1} vs. NiOH/NF:101 mV dec^{-1}) confirmed Volmer-Heyroovsky kinetics with accelerated charge transfer, overall splitting needed just 1.67 V @10 mA cm^{-2}.

Zhao et al., engineered Ir/$Ni(OH)_2$ heterostructures, where robust Ir-$Ni(OH)_2$ synergy stabilized high-valent Ni centers, facilitating O-O coupling for enhanced overall water splitting. (68-69). The Ir/$Ni(OH)_2$ exhibited a higher OER activity, needing only overpotential of 224 mV, whereas the $Ni(OH)_2$ necessitated 437 mV at the benchmark current density. In studies for TWS, the Ir/$Ni(OH)_2$ required merely an additional potential of 262 mV related to the thermodynamically calculated potential. Likewise, Chen et al. have revealed integrating Ru nanoparticles into $Ni(OH)_2$ for hydrogen evolution in alkaline conditions. This material was prepared via spontaneous redox process, driven by the potential differences of the different metallic species, with the entire synthetic process.

6.2. Bimetallic LDHs and Engineered variants as Bifunctional Water-Splitting Electrocatalysts

Layered double hydroxides (LDHs)-versatile 2D nanomaterials-comprise edge-sharing MO_6 octahedral forming continuous nanosheets, with intercalated anions stabilizing the interlayer gallery between brucite-like hydroxide slabs. The simplified chemical formula of LDHs is expressed as $M^{2+}_{1-x}\ .M^{3+}_{x}(OH)_2.(A)^{n-}_{x/n}.yH_2O$ where A^{n-} is the anion intercalated in the LDH layer. M^{3+} and M^{2+} are the trivalent and bivalent cation respectively **(Figure 6)**. Thus, a diverse range of di-, tri or higher-valent cations can be incorporated into LDH layers and by selecting various intercalated anions, interlayer spacing between adjacent brucite-like layers can be precisely tuned. LDHs are often regarded as solid solutions, wherein tri or higher-valent metal ions are homogeneously distributed within $M^{2+}(OH)_2$ matrix (59). Due to adjustable molar ratio of M^{3+} and M^{2+} ions, this would allow a unique layered 2D structure for water splitting application (70). Key advantages of layered double hydroxides (LDHs) for water splitting include:

- 2D sheet-like morphology yields high surface-to-volume ratios, maximizing electro active sites for ions.
- Porous 2D architecture facilitates electrolyte ion diffusion channels.
- Robust interlayer electrostatic interactions confer stability in alkaline media
- Facile synthesis from earth-abundant elements ensures scalability.

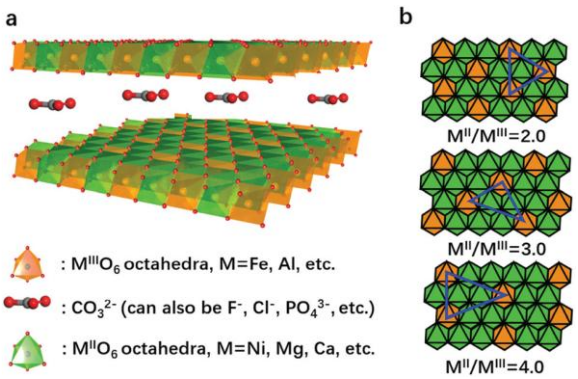

Figure 6: *Structural features of LDHs. Reproduced with permission from reference number 57, Royal Society of Chemistry, 2021.*

In M^{II}-based systems, low-valence metal ions exhibit elevated d-band centers (E_d), serving as preferential OH* adsorption sites under anodic conditions as their valence shifts towards E_F. Higher-valence sites stabilize these oxidized $M^{III/IV}$ forms, facilitating electron transfer. Conversely, under cathodic HER, high-valence ions activate H_2O via strong M-O bonds, enabling subsequent M^{II}-H formation through proton abstraction. Qiu et al., validated this synergy in Ni^{2+}/Fe^{3+}-LDH (71). In HER condition the Fe^{3+} was identified to be the activation center for H_2O to remove activated H* and followed by the formation of Had-$Ni^{\delta+}$.Therefore, regulation or composition variation among different metal ions (M^{II} and M^{III}) lead to modify the interfacial charge dynamics and thereby a paving a new door to modify the electrocatalytic activity. Apart from the basic LDH component (say Ni and Fe in NiFe-LDH) introduction of different foreign cations regulate the charge transfer kinetics. A brief survey on the effect of doping different cation in MII or MIII site lead modify the electron transfer rate as evident from the Figure 7, where a change in Tafel slope value [Δ (Tafel slope)] is monitored. The given survey reflects that the doping of $M_1^{II}$and M_2^{III}in respective M^{II} and M^{III} sites results in improvisation of the charge transfer kinetics. Depending on the position of the MII and M_1^{II}d-band center, the probability of OH* might regulate. The M_1^{II}metal ion with higher d-band center like Fe^{2+}, Mn^{2+}, Co^{2+} (low effective nuclear charge) additionally benefitted the OH* adsorption. Whereas doping of M_2^{III}over MIII site modify the electron transfer by synergistic electron exchange process more prominently. Therefore, from the above example it is evident that LDH are flexible towards not only this doping induced modification but also various other strategical ways like inter-layer spacing modification, vacancy engineering, heterostructure formation etc., to modify the interfacial charge transfer dynamics.

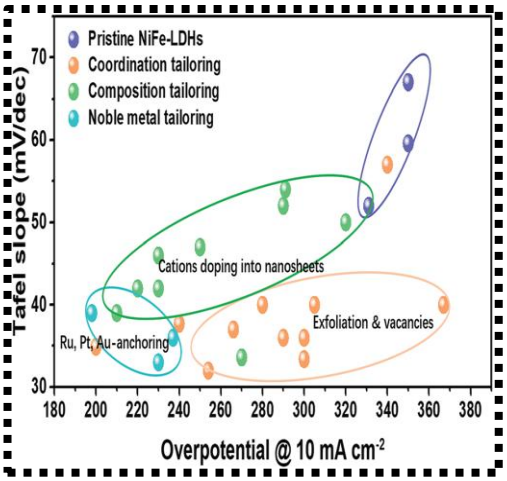

Figure 7: *Summary of the illustrative studies on dressmaking active sites on NiFe-LDHs for improving OER activity. Reproduced with permission from reference number 57, Royal Society of chemistry, 2021.*

The efficacy of active-site engineering strategies for boosting water-splitting performance is evidenced by Tafel slopes and over potentials. As noted, metal hydroxides and bimetallic variants leverage unique structure/morphological features, their 2D nanosheet architecture delivers high surface-to-volume ratios. Beyond 3d transition metal hydroxides, selenides, tellurides, phosphides, and nitrides similarly exhibit robust bifunctional activity (72). Direct synthesis of chalcogenides, phosphides, sulphides, and nitrides from metal salts remains challenging due to morphological complexity. Conversely, structure-preserving chemical transformation of transition metal hydroxides as precursors yields these derivatives more readily, preserving the parent 2D architecture. LDH-derived materials exhibit superior bifunctional water-splitting activity, synergizing layered structures with tailored electronic properties of derivatives. Notably, the metallic conductivity of phosphides/nitrides accelerates interfacial electron transfer.

7. Conclusion and future perspective

Developing efficient catalysts is essential to accelerate water-splitting kinetics at electrode-electrolyte interfaces. Transition metal hydroxides stand out due to their intrinsic activity, earth abundance, stability under anodic potentials, and low cost. Their superior performance arises from optimal electronic structures, 2D Nano sheet morphologies, and corrosion resistance in alkaline media. Here, we summarize recent synthetic strategies for hydroxides and their advances in overall water splitting, while elucidating the fundamental principles, design rationales, and reaction mechanisms. Recent tactics heteroatom engineering, morphological modifications & defect (voids) creation-markedly enhance the catalytic kinetics across the board. Although the performance of metal hydroxides like NiFe-LDH is promising for the Oxygen Evolution Reaction at the laboratory scale, their practical applicability needs to be explored. To design an electrolyzer system, the catalysts need to be stable at high current density (> 500 mA cm^{-2}) for long periods while retaining their structural properties. Moreover, the catalysts need to be synthesized cost-effectively on a larger scale to be compatible with existing commercial devices like Anion Exchange Membrane Water Electrolyzer. Therefore, to connect the gap between existing studies and real time applications for hydrogen evolution, the catalysts need to be made stable for industrial applications.

8. Acknowledgements

S Kundu wish to thank Dr. K Ramesha, Director, CSIR-CECRI for his continuous supports, to Dr. Arun Karmakar, JSPS Postdoctoral fellow, Weseda University, for supporting this review article preparation and Ms. P. Mazumder for formatting the paper. CSIR-CECRI MS reference number # CECRI/PESVC/Pubs./2026-017.

9. References

(1) Garland, N. L.; Papageorgopoulos, D. C.; Stanford, J. M. (2012) Hydrogen and Fuel Cell Technology: Progress, Challenges, and Future Directions. Energy Procedia, 28, 2–11.
(2) Li, X.; Hao, X.; Abudula, A.; Guan, G. (2016) Nanostructured Catalysts for Electrochemical Water Splitting: Current State and Prospects. J. Mater. Chem. A, 4 (31), 11973–12000.
(3) Shafiee, S.; Topal, E. (2009) When Will Fossil Fuel Reserves Be Diminished? Energy Policy, 37 (1), 181–189.
(4) Dincer, I. (2012) Green Methods for Hydrogen Production. Int. J. Hydrogen Energy, 37 (2), 1954–1971.
(5) Anantharaj, S.; Ede, S. R.; Karthick, K.; Sam Sankar, S.; Sangeetha, K.; Karthik, P. E.; Kundu, S. (2018) Precision and Correctness in the Evaluation of Electrocatalytic Water Splitting: Revisiting Activity Parameters with a Critical Assessment. Energy Environ. Sci., 11 (4), 744–771.
(6) Wang, Y.; Yan, D.; El Hankari, S.; Zou, Y.; Wang, S. (2018) Recent Progress on Layered Double Hydroxides and Their Derivatives for Electrocatalytic Water Splitting. Advanced Science.
(7) Jiao, Y.; Zheng, Y.; Jaroniec, M.; Qiao, S. Z. (2015) Design of Electrocatalysts for Oxygen- and Hydrogen-Involving Energy Conversion Reactions. Chem. Soc. Rev. 44 (8), 2060–2086.
(8) Hu, C.; Li, M.; Qiu, J.; Sun, Y. P. (2019) Design and Fabrication of Carbon Dots for Energy Conversion and Storage. Chem. Soc. Rev. 48 (8), 2315–2337.
(9) Debecker, D. P.; Gaigneaux, E. M.; Busca, G. (2009) Exploring, Tuning, and Exploiting the Basicity of Hydrotalcites for Applications in Heterogeneous Catalysis. Chem. - A Eur. J. 15 (16), 3920–3935.
(10) Kumar, K.; Abidat, I.; Canaff, C.; Habrioux, A.; Morais, C.; Napporn, T. W.; Kokoh, K. B. (2018) Metal Loading Effect on the Activity of Co3O4/N-Doped Reduced Graphene Oxide Nanocomposites as Bifunctional Oxygen Reduction/Evolution Catalysts. ChemElectroChem, 5 (3), 483–493.
(11) Shen, X.; Zhang, W.; Liu, W.; Qi, Z.; Jiang, Z.; Yang, J.; Yao, T. (2019) Acidic Oxygen Evolution Reaction. Nat. Commun. No.
(12) Rossmeisl, J.; Dimitrievski, K.; Siegbahn, P.; Nørskov, J. K. (2007) Comparing Electrochemical and Biological Water Splitting. J. Phys. Chem. C, 111 (51), 18821–18823.
(13) Zhou, Y.; Fan, H. J. (2021) Progress and Challenge of Amorphous Catalysts for Electrochemical Water Splitting. ACS Mater. Lett., 3 (1), 136–147.
(14) Madhu, R.; Karmakar, A.; Kumaravel, S.; Sankar, S. S.; Bera, K.; Nagappan, S.; Dhandapani, H. N.; Kundu, S. (2021) Revealing the PH-Universal Electrocatalytic Activity of Co-

Doped RuO 2 toward the Water Oxidation Reaction. ACS Appl. Mater. Interfaces.
(15) Anantharaj, S.; Aravindan, V. (2020) Developments and Perspectives in 3d Transition-Metal-Based Electrocatalysts for Neutral and Near-Neutral Water Electrolysis. Adv. Energy Mater., 10 (1), 1–30.
(16) Fan, K.; Zou, H.; Lu, Y.; Chen, H.; Li, F.; Liu, J.; Sun, L.; Tong, L.; Toney, M. F.; Sui, M.; Yu, J. (2018) Direct Observation of Structural Evolution of Metal Chalcogenide in Electrocatalytic Water Oxidation. ACS Nano, 12 (12), 12369–12379.
(17) Han, N.; Liu, P.; Jiang, J.; Ai, L.; Shao, Z.; Liu, S. (2018) Recent Advances in Nanostructured Metal Nitrides for Water Splitting. J. Mater. Chem. A, 6 (41), 19912–19933.
(18) Kundu, S.; Kumaravel, S.; Karthick, K.; Sankar, S. S.; Karmakar, A.; Madhu, R.; Bera, K. (2021) Recent Progresses in Engineering of Ni and Co Based Phosphides for Effective Electrocatalytic Water Splitting: A Review. ChemElectroChem, 1–49.
(19) Xie, J.; Xie, Y. (2016) Transition Metal Nitrides for Electrocatalytic Energy Conversion: Opportunities and Challenges. Chem. - A Eur. J. 22 (11), 3588–3598.
(20) Kumaravel, S.; Karthick, K.; Sankar, S. S.; Karmakar, A.; Madhu, R.; Bera, K.; Kundu, S. (2021) Current Progressions in Transition Metal Based Hydroxides as Bi-Functional Catalysts towards Electrocatalytic Total Water Splitting. Sustain. Energy Fuels, 5 (24), 6215–6268.
(21) Karmakar, A.; Karthick, K.; Sankar, S. S.; Kumaravel, S.; Madhu, R.; Kundu, S. (2021) A Vast Exploration of Improvising Synthetic Strategies for Enhancing the OER Kinetics of LDH Structures: A Review; Royal Society of Chemistry, Vol. 9.
(22) Nørskov, J. K.; Rossmeisl, J.; Logadottir, A.; Lindqvist, L.; Kitchin, J. R.; Bligaard, T.; Jónsson, H. (2004) Origin of the Overpotential for Oxygen Reduction at a Fuel-Cell Cathode. J. Phys. Chem. B, 108 (46), 17886–17892.
(23) Edwards, P. P.; Kuznetsov, V. L.; David, W. I. F.; Brandon, N. P. (2008) Hydrogen and Fuel Cells: Towards a Sustainable Energy Future. Energy Policy, 36 (12), 4356–4362.
(24) Tahir, M.; Pan, L.; Idrees, F.; Zhang, X.; Wang, L.; Zou, J. J.; Wang, Z. L. (2017) Electrocatalytic Oxygen Evolution Reaction for Energy Conversion and Storage: A Comprehensive Review. Nano Energy, 37 (February), 136–157.
(25) Liu, D.; Yang, Y.; Zhu, H.; Liu, D.; Yan, S.; Zou, Z. (2022) Heat-Electricity Coupling Driven Cascade Oxidation Reaction of Redox Couple and Water. J. Phys. Chem. Lett., 13 (1), 49–57.
(26) Anantharaj, S.; Kundu, S. (2019) Do the Evaluation Parameters Reflect Intrinsic Activity of Electrocatalysts in Electrochemical Water Splitting? ACS Energy Lett., 4 (6), 1260–1264.
(27) Kibsgaard, J.; Chorkendorff, I. (2019) Considerations for the Scaling-up of Water Splitting Catalysts. Nat. Energy, 4 (6), 430–433.
(28) Anantharaj, S.; Karthik, P. E.; Noda, S. (2021) The Significance of Properly Reporting Turnover Frequency in Electrocatalysis Research. Angew. Chemie - Int. Ed., 60 (43), 23051–23067.
(29) Wang, Y.; Xie, C.; Liu, D.; Huang, X.; Huo, J.; Wang, S. (2016) Nanoparticle-Stacked Porous Nickel-Iron Nitride Nanosheet: A Highly Efficient Bifunctional Electrocatalyst for Overall Water Splitting. ACS Appl. Mater. Interfaces, 8 (29), 18652–18657.
(30) Tamilselvan, A.; Balakumar, S.; Sakar, M.; Nayek, C.; Murugavel, P.; Saravana Kumar, K. (2014) Role of Oxygen Vacancy and Fe-O-Fe Bond Angle in Compositional, Magnetic, and Dielectric Relaxation on Eu-Substituted BiFeO3 Nanoparticles. Dalt. Trans., 43 (15), 5731–5738.
(31) Zhang, J. Y.; Yan, Y.; Mei, B.; Qi, R.; He, T.; Wang, Z.; Fang, W.; Zaman, S.; Su, Y.; Ding, S.; Xia, B. Y. (2021) Local Spin-State Tuning of Cobalt-Iron Selenide Nanoframes for the Boosted Oxygen Evolution. Energy Environ. Sci, 14 (1), 365–373.
(32) Harzandi, A. M.; Shadman, S.; Nissimagoudar, A. S.; Kim, D. Y.; Lim, H. D.; Lee, J. H.; Kim, M. G.; Jeong, H. Y.; Kim, Y.; Kim, K. S. (2021) Ruthenium Core–Shell Engineering with Nickel Single Atoms for Selective Oxygen Evolution via Nondestructive Mechanism. Adv. Energy Mater., 11 (10), 1–12.
(33) Suntivich, J.; May, K. J.; Gasteiger, H. A.; Goodenough, J. B.; Shao-Horn, Y. (2011) A Perovskite Oxide Optimized for Oxygen Evolution Catalysis from Molecular Orbital Principles. Science (80). 334 (6061), 1383–1385.
(34) Yan, Y.; Xia, B.; Xu, Z.; Wang, X. (2014) Recent Development of Molybdenum Sulfides as Advanced Electrocatalysts for Hydrogen Evolution Reaction. ACS Catal., 4 (6), 1693–1705.
(35) Safizadeh, F.; Ghali, E.; Houlachi, G. (2015) Electrocatalysis Developments for Hydrogen Evolution Reaction in Alkaline Solutions - A Review. Int. J. Hydrogen Energy, 40 (1), 256–274.
(36) Mahmood, N.; Yao, Y.; Zhang, J. W.; Pan, L.; Zhang, X.; Zou, J. J. (2018) Electrocatalysts for Hydrogen Evolution in Alkaline Electrolytes: Mechanisms, Challenges, and Prospective Solutions. Adv. Sci., 5 (2).
(37) Karmakar, A.; Karthick, K.; Kumaravel, S.; Sankar, S. S.; Kundu, S. (2021) Enabling and Inducing Oxygen Vacancies in Cobalt Iron Layer Double Hydroxide via Selenization as Precatalysts for Electrocatalytic Hydrogen and Oxygen Evolution Reactions. Inorg. Chem., 60 (3), 2023–2036.
(38) Liu, Q.; Huang, J.; Zhao, Y.; Cao, L.; Li, K.; Zhang, N.; Yang, D.; Feng, L.; Feng, L. (2019) Tuning the Coupling Interface of Ultrathin Ni 3 S 2 @NiV-LDH Heterogeneous Nanosheet Electrocatalysts for Improved Overall Water Splitting. Nanoscale, 11 (18), 8855–8863.
(39) Anantharaj, S.; Noda, S. (2020) Nickel Selenides as Pre-Catalysts for Electrochemical Oxygen Evolution Reaction: A Review. Int. J. Hydrogen Energy, 45 (32), 15763–15784.
(40) Dionigi, F.; Strasser, P. (2016) NiFe-Based (Oxy)Hydroxide Catalysts for Oxygen Evolution Reaction in Non-Acidic Electrolytes. Adv. Energy Mater., 6 (23).
(41) Wang, Y.; Qiao, M.; Li, Y.; Wang, S. (2018) Tuning Surface Electronic Configuration of NiFe LDHs Nanosheets by Introducing Cation Vacancies (Fe or Ni) as Highly Efficient Electrocatalysts for Oxygen Evolution Reaction. Small, 14 (17), 1–6.
(42) Chen, G.; Wang, T.; Zhang, J.; Liu, P.; Sun, H.; Zhuang, X.; Chen, M.; Feng, X. (2018) Accelerated Hydrogen Evolution Kinetics on NiFe-Layered Double Hydroxide Electrocatalysts by Tailoring Water Dissociation Active Sites. Adv. Mater., 30 (10), 1–7.
(43) Chen, J. Y. C.; Dang, L.; Liang, H.; Bi, W.; Gerken, J. B.; Jin, S.; Alp, E. E.; Stahl, S. S. (2015) Operando Analysis of NiFe and Fe Oxyhydroxide Electrocatalysts for Water Oxidation: Detection of Fe4+ by Mössbauer Spectroscopy. J. Am. Chem. Soc., 137 (48), 15090–15093.
(44) Qiao, X.; Kang, H.; Li, Y.; Cui, K.; Jia, X.; Liu, H.; Qin, W.; Pupucevski, M.; Wu, G. (2020) Porous Fe-Doped β-Ni(OH)2Nanopyramid Array Electrodes for Water Splitting. ACS Appl. Mater. Interfaces, 12 (32), 36208–36219.
(45) Ren, J. T.; Yuan, G. G.; Weng, C. C.; Chen, L.; Yuan, Z. Y. (2018) Uniquely Integrated Fe-Doped Ni(OH)2 Nanosheets for Highly Efficient Oxygen and Hydrogen Evolution Reactions. Nanoscale, 10 (22), 10620–10628.
(46) Zhao, G.; Li, P.; Cheng, N.; Dou, S. X.; Sun, W. (2020) An Ir/Ni(OH)2 Heterostructured Electrocatalyst for the Oxygen Evolution Reaction: Breaking the Scaling Relation, Stabilizing Iridium(V), and Beyond. Adv. Mater., 32 (24), 1–9.
(47) Chen, Q. Q.; Yang, X.; Hou, C. C.; Li, K.; Chen, Y. (2019) Inlay of Ultrafine Ru Nanoparticles into a Self-Supported Ni(OH)2 Nanoarray for Hydrogen Evolution with Low Overpotential and Enhanced Kinetics. J. Mater. Chem. A, 7 (18), 11062–11068.
(48) Lv, C.; Wang, X.; Gao, L.; Wang, A.; Wang, S.; Wang, R.; Ning, X.; Li, Y.; Boukhvalov, D. W.; Huang, Z.; Zhang, C. (2020) Triple Functions of Ni(OH)2on the Surface of WN Nanowires Remarkably Promoting Electrocatalytic Activity in Full Water Splitting. ACS Catal., 10 (22), 13323–13333.

(49) Jiang, J.; Tang, Y.; Dong, L.; Zhang, W.; Wu, H.; Yu, X. Y. (2020) Plasma-Reduced Co(OH)2with Activated Hydrogen Evolution and Overall Water Splitting Performance. Sustain. Energy Fuels, 4 (6), 2645–2649.
(50) Wang, Y.; Yang, Y.; Wang, X.; Li, P.; Shao, H.; Li, T.; Liu, H.; Zheng, Q.; Hu, J.; Duan, L.; Hu, C.; Liu, J. (2020) Electro-Synthesized Co(OH)2@CoSe with Co-OH Active Sites for Overall Water Splitting Electrocatalysis. Nanoscale Adv., 2 (2), 792–797.
(51) Saraj, C. S.; Singh, S. C.; Shukla, A.; Yu, W.; Fayyaz, M. U.; Guo, C. (2021) single-Step and Sustainable Fabrication of Ni(OH)2/Ni Foam Water Splitting Catalysts via Electric Field Assisted Pulsed Laser Ablation in Liquid. ChemElectroChem, 8 (1), 209–217.
(52) Du, X.; Yang, Z.; Li, Y.; Gong, Y.; Zhao, M. (2018) Controlled Synthesis of Ni(OH)2/Ni3S2 Hybrid Nanosheet Arrays as Highly Active and Stable Electrocatalysts for Water Splitting. J. Mater. Chem. A, 6 (16), 6938–6946.
(53) Xi, W.; Yan, G.; Tan, H.; Xiao, L.; Cheng, S.; Khan, S. U.; Wang, Y.; Li, Y. (2018) Superaerophobic P-Doped Ni(OH)2/NiMoO4 Hierarchical Nanosheet Arrays Grown on Ni Foam for Electrocatalytic Overall Water Splitting. Dalt. Trans., 47 (26), 8787–8793.
(54) Yan, J.; Kong, L.; Ji, Y.; White, J.; Li, Y.; Zhang, J.; An, P.; Liu, S.; Lee, S. T.; Ma, T. (2019) Single Atom Tungsten Doped Ultrathin α-Ni(OH)2 for Enhanced Electrocatalytic Water Oxidation. Nat. Commun., 10 (1), 1–10.
(55) Liu, S.; Gao, R. T.; Sun, M.; Wang, Y.; Nakajima, T.; Liu, X.; Zhang, W.; Wang, L. (2021) In Situ Construction of Hybrid Co(OH)2 Nanowires for Promoting Long-Term Water Splitting. Appl. Catal. B Environ, 292 (October 2020).
(56) Wang, Z.; Ji, S.; Liu, F.; Wang, H.; Wang, X.; Wang, Q.; Pollet, B. G.; Wang, R. (2019) Highly Efficient and Stable Catalyst Based on Co(OH)2@Ni Electroplated on Cu-Metallized Cotton Textile for Water Splitting. ACS Appl. Mater. Interfaces, 11 (33), 29791–29798.
(57) Zhou, D.; Li, P.; Lin, X.; McKinley, A.; Kuang, Y.; Liu, W.; Lin, W. F.; Sun, X.; Duan, X. (2021) Layered Double Hydroxide-Based Electrocatalysts for the Oxygen Evolution Reaction: Identification and Tailoring of Active Sites, and Superaerophobic Nanoarray Electrode Assembly. Chem. Soc. Rev., 50 (15), 8790–8817.
(58) Wang, Y.; Qiao, M.; Li, Y.; Wang, S. (2018) Tuning Surface Electronic Configuration of NiFe LDHs Nanosheets by Introducing Cation Vacancies (Fe or Ni) as Highly Efficient Electrocatalysts for Oxygen Evolution Reaction. Small, 14 (17), 1–6.
(59) Song, F.; Hu, X. (2014) Exfoliation of Layered Double Hydroxides for Enhanced Oxygen Evolution Catalysis. Nat. Commun., 5, 1–9.
(60) Chen, L.; Zhang, H.; Chen, L.; Wei, X.; Shi, J.; He, M. (2017) Facile Synthesis of Cu Doped Cobalt Hydroxide (Cu-Co(OH)2) Nano-Sheets for Efficient Electrocatalytic Oxygen Evolution. J. Mater. Chem. A, 5 (43), 22568–22575.
(61) Cai, Z.; Zhou, D.; Wang, M.; Bak, S.; Wu, Y.; Wu, Z.; Tian, Y.; Xiong, X.; Li, Y.; Liu, W.; Siahrostami, S.; Kuang, Y.; Yang, X.; Duan, H.; Feng, Z.; Wang, H.; Sun, X. (2018) Introducing Fe 2+ into Nickel–Iron Layered Double Hydroxide: Local Structure Modulated Water Oxidation Activity . Angew. Chemie, 130 (30), 9536–9540.
(62) Fan, K.; Chen, H.; Ji, Y.; Huang, H.; Claesson, P. M.; Daniel, Q.; Philippe, B.; Rensmo, H.; Li, F.; Luo, Y.; Sun, L. (2016) Nickel-Vanadium Monolayer Double Hydroxide for Efficient Electrochemical Water Oxidation. Nat. Commun., 7 (May), 1–9.
(63) Koishi, T.; Yasuoka, K.; Fujikawa, S.; Zeng, X. C. (2011) Measurement of Contact-Angle Hysteresis for Droplets on Nanopillared Surface and in the Cassie and Wenzel States: A Molecular Dynamics Simulation Study. ACS Nano, 5 (9), 6834–6842.
(64) Zhao, D.; Jiang, K.; Pi, Y.; Huang, X. (2017) Superior Electrochemical Oxygen Evolution Enabled by Three-Dimensional Layered Double Hydroxide Nanosheet Superstructures. ChemCatChem, 9 (1), 84–88.
(65) Liu, R.; Wang, Y.; Liu, D.; Zou, Y.; Wang, S. (2017) Water-Plasma-Enabled Exfoliation of Ultrathin Layered Double Hydroxide Nanosheets with Multivacancies for Water Oxidation. Adv. Mater., 29 (30), 1–7.
(66) Song, F.; Hu, X. (2014) Ultrathin Cobalt − Manganese Layered Double Hydroxide Is An. J. Am. Chem. Soc., 1–4.
(67) Nadeema, A.; Dhavale, V. M.; Kurungot, S. (2017) NiZn Double Hydroxide Nanosheet-Anchored Nitrogen-Doped Graphene Enriched with the γ-NiOOH Phase as an Activity Modulated Water Oxidation Electrocatalyst. Nanoscale, 9 (34), 12590–12600.
(68) Ma, W.; Ma, R.; Wu, J.; Sun, P.; Liu, X.; Zhou, K.; Sasaki, T. (2016) Development of Efficient Electrocatalysts: Via Molecular Hybridization of NiMn Layered Double Hydroxide Nanosheets and Graphene. Nanoscale, 8 (19), 10425–10432.
(69) Qiao, C.; Zhang, Y.; Zhu, Y.; Cao, C.; Bao, X.; Xu, J. (2015) One-Step Synthesis of Zinc-Cobalt Layered Double Hydroxide (Zn-Co-LDH) Nanosheets for High-Efficiency Oxygen Evolution Reaction. J. Mater. Chem. A, 3 (13), 6878–6883.
(70) Nai, J.; Yin, H.; You, T.; Zheng, L.; Zhang, J.; Wang, P.; Jin, Z.; Tian, Y.; Liu, J.; Tang, Z.; Guo, L. (2015) Efficient Electrocatalytic Water Oxidation by Using Amorphous Ni-Co Double Hydroxides Nanocages. Adv. Energy Mater., 5 (10), 1–7.
(71) Qiu, Z.; Tai, C. W.; Niklasson, G. A.; Edvinsson, T. (2019) Direct Observation of Active Catalyst Surface Phases and the Effect of Dynamic Self-Optimization in NiFe-Layered Double Hydroxides for Alkaline Water Splitting. Energy Environ. Sci., 12 (2), 572–581.
(72) Jin, S. (2017) Are Metal Chalcogenides, Nitrides, and Phosphides Oxygen Evolution Catalysts or Bifunctional Catalysts? ACS Energy Lett., 2 (8), 1937–1938.

9. About the author(s)

Dr. Subrata Kundu earned his Ph.D. from Indian Institute of Technology (IIT), Kharagpur, India, in early 2005. He conducted postdoctoral research at the University of Nebraska, Lincoln, USA and Texas A&M University, College Station, Texas, USA (2005-2023), Dr. Kundu was awarded FRSC from London and has been an associate editor for the renowned 'Journal of Material Chemistry A' and 'Materials Advances' (RSC publishers) since 2022, as well as 'Scientific Reports' (Nature Group Publishers) since 2015.He was recently named to the Editorial Advisory Board of the esteemed 'ACS Applied Materials & Interfaces' (ACS) and Inorganic Chemistry Frontiers (RSC). Dr. Kundu and his team lead cutting-edge in material science, focusing on energy, environment, catalysis, and electrocatalysis applications.

Article Note: A collection of invited papers based on *Award Lecture* presentations in the 22nd CRS® International Symposium *'Rasayan 22'* held at the Visvesvaraya Technological University (VTU), Muddenahalli, Chikkaballapur, Karnataka, India during January 8-10, 2026.